AD-A052 167 GENERAL APPLIED SCIENCE LABS INC WESTBURY N Y F/G 20/4
AN INVESTIGATION OF WALL AND BACK PRESSURE EFFECTS IN TRANSONIC--ETC(U)
JUN 77 S ELZWEIG, P BARONTI N00014-76-C-0149
UNCLASSIFIED GASL-TR-245 NL

1 OF 1
ADA
052167

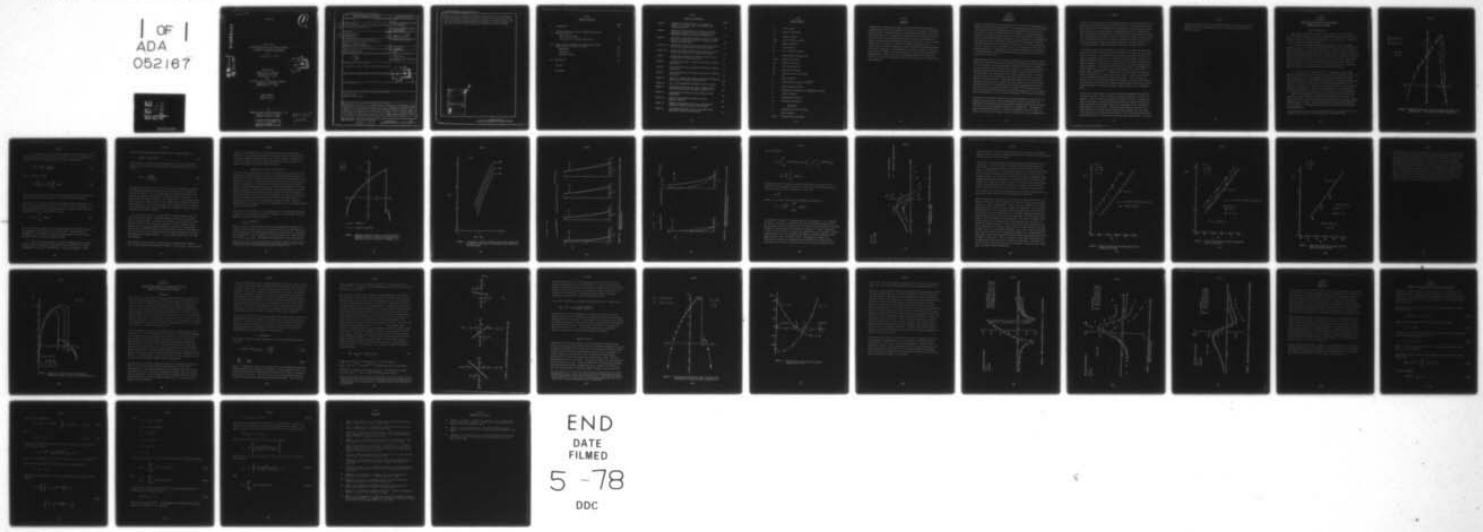

END
DATE
FILMED
5 -78
DDC

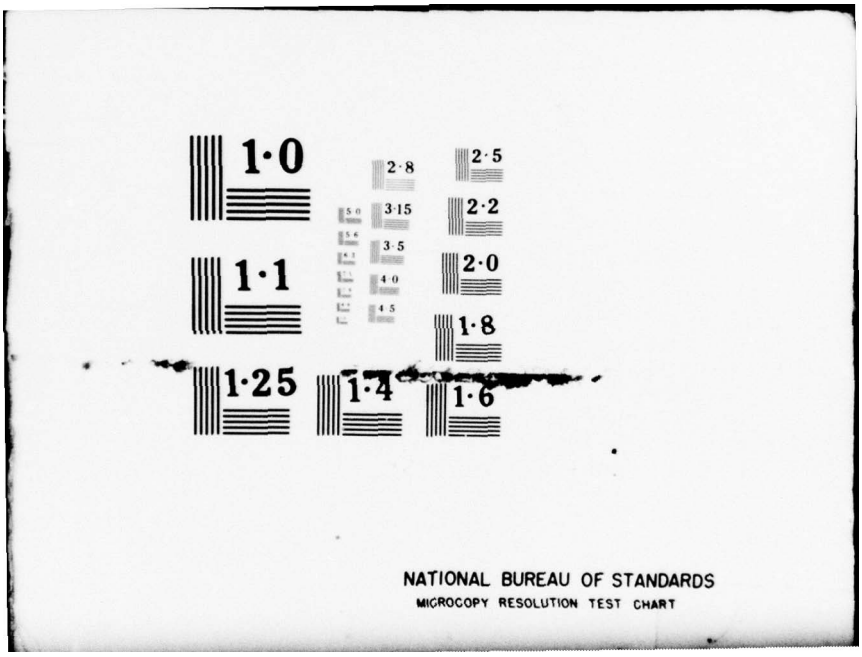
1·0
1·1
1·25
1·4
1·6
1·8
2·0
2·2
2·5
2·8
3·15
3·5
4·0
4·5
5·0
5·6
NATIONAL BUREAU OF STANDARDS
MICROCOPY RESOLUTION TEST CHART

Recorded

JUNE 1977

GASL TR 245

AN INVESTIGATION OF WALL AND BACK PRESSURE EFFECTS IN TRANSONIC INTERFERENCE

By

S. Elzweig & P. Baronti

PREPARED FOR

OFFICE OF NAVAL RESEARCH
DEPARTMENT OF THE NAVY
ARLINGTON, VA 22217

AND

AIR FORCE OFFICE OF SCIENTIFIC RESEARCH
BOLLING AIR FORCE BASE
WASHINGTON, D. C. 20332

UNDER CONTRACT

N00014-76-C-0149

By

GENERAL APPLIED SCIENCE LABORATORIES, INC.
Merrick and Stewart Avenues
Westbury, New York 11590

C61-205
6/15/77

UNCLASSIFIED
SECURITY CLASSIFICATION OF THIS PAGE (When Data Entered)

REPORT DOCUMENTATION PAGE

READ INSTRUCTIONS BEFORE COMPLETING FORM

1. REPORT NUMBER
2. GOVT ACCESSION NO.
3. RECIPIENT'S CATALOG NUMBER

4. TITLE (and Subtitle)
An Investigation of Wall and Back Pressure Effects in Transonic Interference.

5. TYPE OF REPORT & PERIOD COVERED
Final Report.

6. PERFORMING ORG. REPORT NUMBER
GASL-TR-245

7. AUTHOR(s)
Sheldon/Elzweig
Paolo/Baronti

8. CONTRACT OR GRANT NUMBER(s)
N00014-76-C-0149

9. PERFORMING ORGANIZATION NAME AND ADDRESS
General Applied Science Laboratories, Inc
Merrick & Stewart Avenues
Westbury, New York 11590

10. PROGRAM ELEMENT, PROJECT, TASK AREA & WORK UNIT NUMBERS

11. CONTROLLING OFFICE NAME AND ADDRESS
Office of Naval Research, Department of the Navy
800 N. Quincy Street
Arlington, VA 22217

12. REPORT DATE
June 1977

13. NUMBER OF PAGES
32

14. MONITORING AGENCY NAME & ADDRESS (if different from Controlling Office)
44p.

15. SECURITY CLASS. (of this report)
UNCLASSIFIED

15a. DECLASSIFICATION/DOWNGRADING SCHEDULE

16. DISTRIBUTION STATEMENT (of this Report)

Approved for public release; distribution unlimited.

17. DISTRIBUTION STATEMENT (of the abstract entered in Block 20, if different from Report)

18. SUPPLEMENTARY NOTES

19. KEY WORDS (Continue on reverse side if necessary and identify by block number)

Transonic Flow
Transonic Interference

20. ABSTRACT (Continue on reverse side if necessary and identify by block number)

An approximate method for the determination of tunnel wall interference on two-dimensional non-lifting supercritical airfoils is presented. The method assumes classical linearized subsonic interference theory applied to an airfoil whose thickness is increased so as to match the far field transonic velocity potential. The interference potential at the wing trailing edge is ta[illegible] as the parameter controlling the shock location on the airfoil. Sample computations of circular arc airfoils in tunnels with solid, porous and slotted walls are shown to

DD FORM 1 JAN 73 1473 EDITION OF 1 NOV 65 IS OBSOLETE
146 800

UNCLASSIFIED
SECURITY CLASSIFICATION OF THIS PAGE (When Data Entered)

adequately predict the shock displacement produced by the wall constraints. Also presented is a numerical analysis, based on a shock fitting technique, for the determination of exact shape and location of imbedded shocks. With the analysis and accompanying numerical code some results are provided to show the sensitivity of back pressure perturbations on shock location.

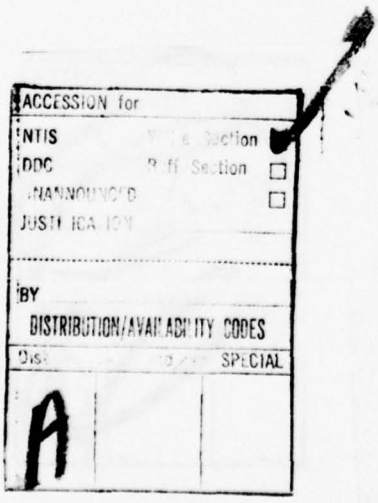

TABLE OF CONTENTS

LIST OF ILLUSTRATIONS

LIST OF SYMBOLS

c	airfoil chord
c_p	pressure coefficient
D	doublet strength
$F(x)$	airfoil profile function
h	tunnel semi-height
K	slot parameter
M_∞	free stream Mach number
r	decay function, Equation (4)
$T=1/R$	porosity parameters
u,v	velocity components
U_∞	free stream velocity
x,y	Cartesian coordinates
x_s	location of shock on airfoil
α	angle of attack
β	compressibility factor, $(1-M_\infty^2)^{1/2}$
γ	ratio of specific heats
ξ	stretched x-coordinate (in computational space)
τ	airfoil thickness
ϕ	perturbation potential
ϕ'	interference potential

Subscripts

0	conditions at airfoil surface
s	shock location
LE,TE	leading and trailing edge

ABSTRACT

An approximate method for the determination of tunnel wall interference on two-dimensional non-lifting supercritical airfoils is presented. The method assumes classical linearized subsonic interference theory applied to an airfoil whose thickness is increased so as to match the far field transonic velocity potential. The interference potential at the wing trailing edge is taken as the parameter controlling the shock location on the airfoil. Sample computations of circular arc airfoils in tunnels with solid, porous and slotted walls are shown to adequately predict the shock displacement produced by the wall constraints. Also presented is a numerical analysis, based on a shock fitting technique, for the determination of exact shape and location of imbedded shocks. With the analysis and accompanying numerical code some results are provided to show the sensitivity of back pressure perturbations on shock location.

SECTION I
INTRODUCTION

Since the early 1970's, with the development of the numerical computation techniques initiated by Murman and Coles[1], it has been possible to study numerically the transonic flow field around more and more complex configurations in free-air as well as within the confinements of wind tunnels. At the same time, a method for assessing the presence and level of wall interference in transonic tests, and for eliminating this interference by an adjustment of wall conditions, was suggested by Ferri and Baronti[2] and by Sears[3]. More recently, Kemp[4] has introduced the concept of "correctable" interference, for the direct determination of transonic tunnel corrections. Thus, by a combination of analyses and testing techniques, it would appear that significant advances can be expected in developing means for recognizing, measuring and possibly eliminating transonic tunnel interference.

Although some progress in wall correction techniques has been reported, noticeably in the experiments performed at Calspan[5], the procedure based on "adaptive" or "self-correcting" walls appears rather complex and difficult to implement. On the other hand, systematic numerical computations of flow fields around aerodynamic configurations in free-air and in tunnels can indicate the presence of interference. The computations are, however, lengthy, and do not directly yield the level of wall interference and tunnel corrections as in classical subsonic interference theory. The direct determination of wall interference and tunnel corrections for transonic conditions (subcritical as well as supercritical) would be, on the other hand, very useful as recognized and pursued analytically in the work performed by Lo and Kraft[6,7,8] at AEDC, and in the work performed by Kemp[4], which combines numerical computations with wind tunnel pressure measurements at the wall and at the model to infer tunnel corrections.

An approach which contains some of the concepts developed by Kraft and Lo, and which intends to provide a direct determination of tunnel interference by a combination of approximate analytical methods and tunnel measurements, has been the subject of an investigation at GASL and is reported here. The method is based on the observation that for certain wing profiles such as circular arc airfoils at zero angle of attack, the wall interference is mostly manifested by

a shift of the shock position, with minor alteration of the wing pressure distribution upstream and downstream of the shock, and by a corresponding variation, with respect to free-air conditions, of the potential at the wing trailing edge. This variation can be calculated with reasonable accuracy by a standard subsonic interference method, based on the Prandtl-Glauert scaling rule and applied to a thicker wing profile which satisfies the far field transonic velocity potential. The method is applied to circular arc profiles at zero angle of attack in tunnels with solid, porous and slotted walls and is shown to provide, in a first approximation, a good indication of wall effect on shock position.

In a parallel effort, also described in this report, an attempt has been made to assess the effects of back pressure on pressure distribution and shock location on an airfoil. The effects of back pressure and/or axial pressure gradients on model characteristics, in particular on shock location, have been recognized repeatedly, for instance in connection with the boattail drag of axisymmetric models.[9] Similarly, back pressure effects were held responsbile for the displacement of shock location on circular arc airfoils from expected free flight conditions, in a series of experiments conducted in a joint effort between GASL and WPAFB,[10,11]. The determination of the effects of small back pressure perturbations on shock location does, however, require the availability of an accurate procedure for locating the shock. In this respect, an analysis (and a special computer code) which employs a shock fitting technique and which satisfies exactly the transonic Rankine-Hugoniot shock jump relation, has been developed to determine the exact shape and location of an embedded shock.

The analysis is an extension of concepts previously developed by Murman[12] and by Hafez and Cheng[13]. More refinement is however obtained with the present procedure. With the shock point operator of Murman the shock is smeared over several grid points; with the shock fitting technique of Hafez and Cheng the shock jump relations are applied between two contiguous points, and the exact shock location is not provided. The present code, however, determines the exact position of the shock between neighboring grid points and, thus allows for a more precise evaluation of the effects of small external perturbation on shock location, even in the case of relatively course grid networks. A discus-

sion of the analysis and of the numerical algorithm, and sample computations showing the effect of back pressure on shock location, are presented in a following section.

SECTION II

APPROXIMATE ANALYSIS OF WALL INTERFERENCE EFFECTS ON SHOCK LOCATION

Basic Considerations

The proposed procedure for inferring the effects of wall interference on shock location is based on a number of sequential steps each of which may contain certain physical assumptions and mathematical approximations. Each step is now discussed in a sequential manner.

1. A basic assumption underlying the procedure is that, in certain transonic tests of non-lifting, two-dimensional airfoils, wall interference will mainly change the position of the shock and only slightly* the distribution of pressure upstream and downstream of the shock. Such a situation is typified by the result of Figure (1), taken from the experiments of Reference (14), which show the pressure distribution over an airfoil in a tunnel with slotted walls. The data along curve (a) are considered interference-free (small model with respect to tunnel dimensions), whereas the data of curve (b) are affected by wall interference with a consequent upstream shift of the shock.

2. The second step of the procedure is to postulate that the shock position on the airfoil is known and that the pressure distribution, before and aft the shock, can be either computed by an approximate analytical method (the method of Spreiter and Alksne[15] for both the accelerating and decelerating portions of the flow has been used in the computations performed here for circular arc airfoils), or that this pressure distribution is the one directly measured in an experiment. (The fact that experimental results may contain wall interference does not detract from the overall logic of the procedure.)

Then, by integration of the pressure over the airfoil for several shock locations, a unique functional relationship between the shock location, x_s, and the difference of the perturbation velocity potential, $\Delta\phi=\phi_{TE}-\phi_{LE}$, between leading and trailing edge can be established for any given Mach number and airfoil geometry. This relationship is held to be true for both unconfined and confined flows.

---

*Further qualifications to this statement will be provided below.

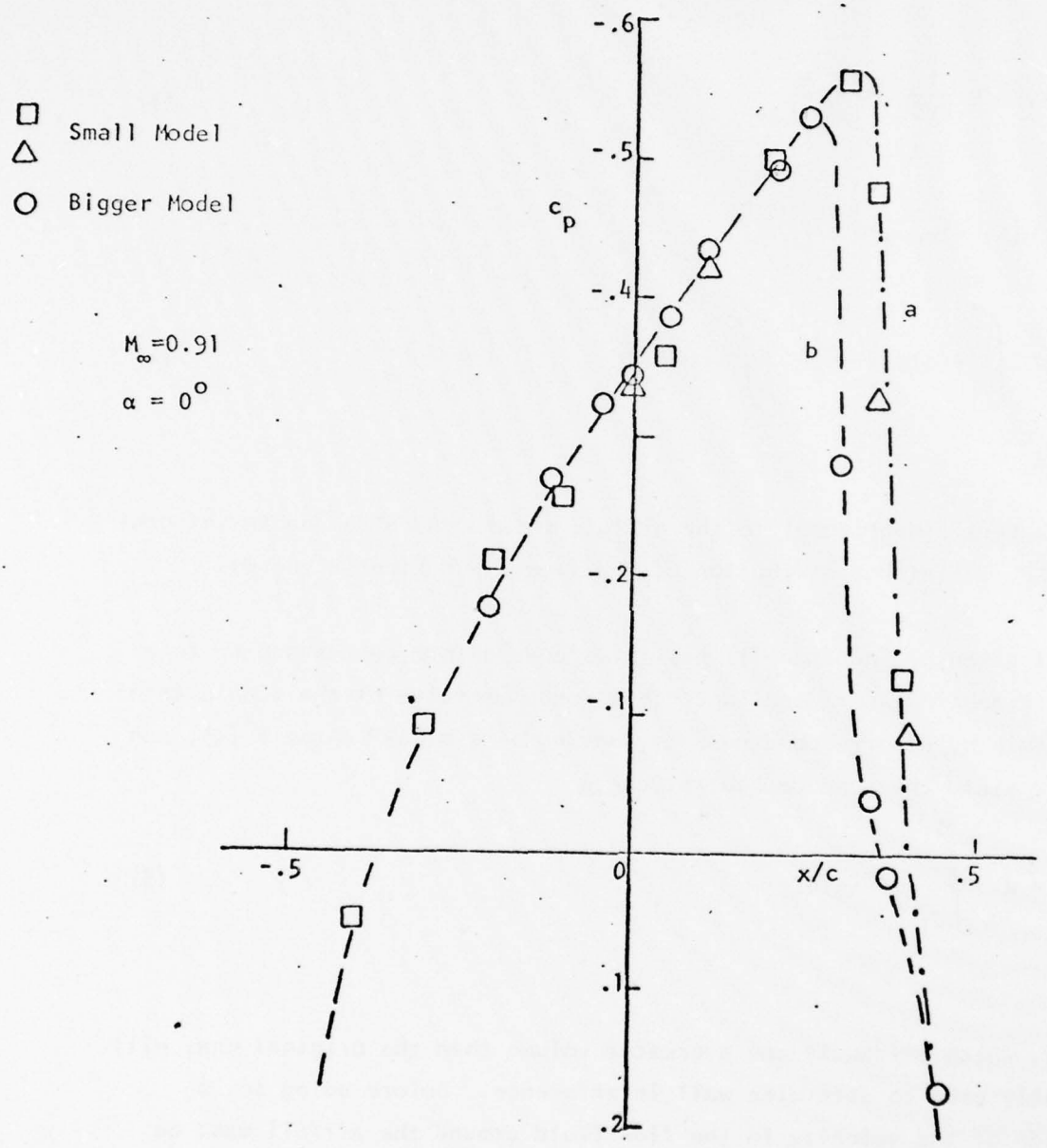

FIGURE 1. PRESSURE DISTRIBUTION OVER A 6% CIRCULAR ARC AIRFOIL IN A SLOTTED TUNNEL. EXPERIMENTAL DATA FROM REFERENCE (14).

3. The next step is to calculate the transonic far field potential from the known pressure distribution over the airfoil. As has been established in Reference (1), the far field potential of a non-lifting airfoil is

$$\phi(x,y) = \frac{1}{2\pi\beta} \; D \; \frac{x}{x^2+\beta^2 y^2} \tag{1}$$

where the doublet strength

$$D = 2\int_{-1}^{1} F(\xi)\,d\xi + \frac{\gamma+1}{2} \iint_{\infty}^{\infty} u^2\,d\xi\,d\zeta \tag{2}$$

consists of a term proportional to the airfoil volume and of a double integral containing the nonlinear contribution of the flow field kinetic energy.

The potential given by Equation (1) has the standard form corresponding to a doublet with Prandtl-Glauert scaling. Thus, once the value of the double integral is determined, a corresponding body, having a "similar" shape $F^*(\xi)$, can be defined to yield the same doublet strength

$$D = 2 \int_{-1}^{1} F^*(\xi)\,d\xi \tag{3}$$

The new body, which evidently has a greater volume than the original one, will be subsequently used to determine wall interference. Before doing so, a representation of the velocity in the flow field around the airfoil must be provided in order to compute the double integral.

4. Since the early, approximate, analytical methods based on the Green theorem, such as the method of developed by Spreiter and Alksne[16], rational representations of the mid field velocity, u, have been suggested. Among

these is the approximation used by Kraft[7] in his integral method, i.e.,

$$u(x,y) = u(x,0)\ e^{-y/r}, \tag{4}$$

relating the mid field velocity to the velocity on the airfoil, with the parameter r(x) satisfying the irrotationality condition on the airfoil and given by

$$r(x) = -\frac{u(x,0)}{(\partial u/\partial y)_{x,0}} \tag{5}$$

The approximation implies that u is equal to zero in the regions upstream of the leading edge and downstream of the trailing edge. Also, it cannot be correct for negative r, since it would imply an expotential increase of the perturbation velocity from the airfoil outwards; however, by taking in Equation (4) the absolute value of r, for regions where $r<0$, the proper decay can be recovered. These inaccuracies are recognized as conceptual limitations ofthe approximation. The errors that application of Equation (4) may produce in the present context is however thought to be acceptable and such as to not invalidate the solution procedure.

5. With the new airfoil of shape $F^{*}(\xi)$, satisfying Equation (3), subsonic linear interference, with Prandtl-Glauert scaling, is now invoked. The new (thicker) airfoil is assumed to be placed in a wind tunnel with either solid or ventilated walls (porous and slotted of infinite length), and the perturbation $\Delta\phi' = \phi'_{TE} - \phi'_{LE}$ produced by the wall constraints is calculated. (Details of the calculation for non-lifting airfoils are given in the Appendix.) This value of $\Delta\phi'$ is then added linearily to the value $\Delta\phi$ determineed in Step 1, and from the relationship relating x_s to $\Delta\phi$, the new position of the shock is determined.

The procedure can be utilized in a direct manner to determine the expected shift in shock position when placing an airfoil in a wind tunnel. More rewarding,

however, is the application of the procedure to wind tunnel airfoil data. Indeed, by the experimentally determined pressure distribution on the airfoil it will be possible, by following the steps indicated above, to determine the value of $\Delta\phi'$ induced by the tunnel wall constraints and then the amount of shock displacement caused by the wall interference.

Application to a Circular Arc Airfoil

The pressure distribution over a circular arc airfoil under supercritical flow conditions is obtained by applying the local linearization method of Spreiter and Alksne[15]. For an assumed shock position, the pressure distribution in front and behind the shock is obtained by applying the accelerating and decelerating solution, respectively. Accelerating and decelerating solutions are matched at the shock by assuming that the shock is normal and by satisfying the normal shock jump relations. Shown in Figure (2) is a comparison between a numerical solution* and the Spreiter-Alksne solution (with the shock position taken to be the one obtained with the numerical computation). The Spreiter-Alksne solution is then used to determine, in function of free-stream Mach number, the difference in potential, $\Delta\phi$, between leading and trailing edge in terms of shock locations x_s. Typical results, for representative free-stream Mach numbers, are plotted in Figure (3).

The next step of the procedure is to compute the far field potential, Equations (1 and 2). For a circular arc airfoil of thickness τ, the mid field velocity, Equations (4 and 5), can be written as

$$u = u_o \, e^{-4\tau y/|u_o|},$$

where $u = -c_p/2$. As shown in Figure (4,a), this approximation reproduces very accurately the numerical results over the portion of the wing with negative c_p. In the regions near the airfoil nose and behind the shock, where c_p is positive, the approximation is still acceptable, as shown in Figure (4,b), when the absolute value of u_0 is taken. The strength of the doublet D is then provided by

*Numerical solutions have been obtained with the GASL transonic program, which includes the shock fitting technique discussed in Section III.

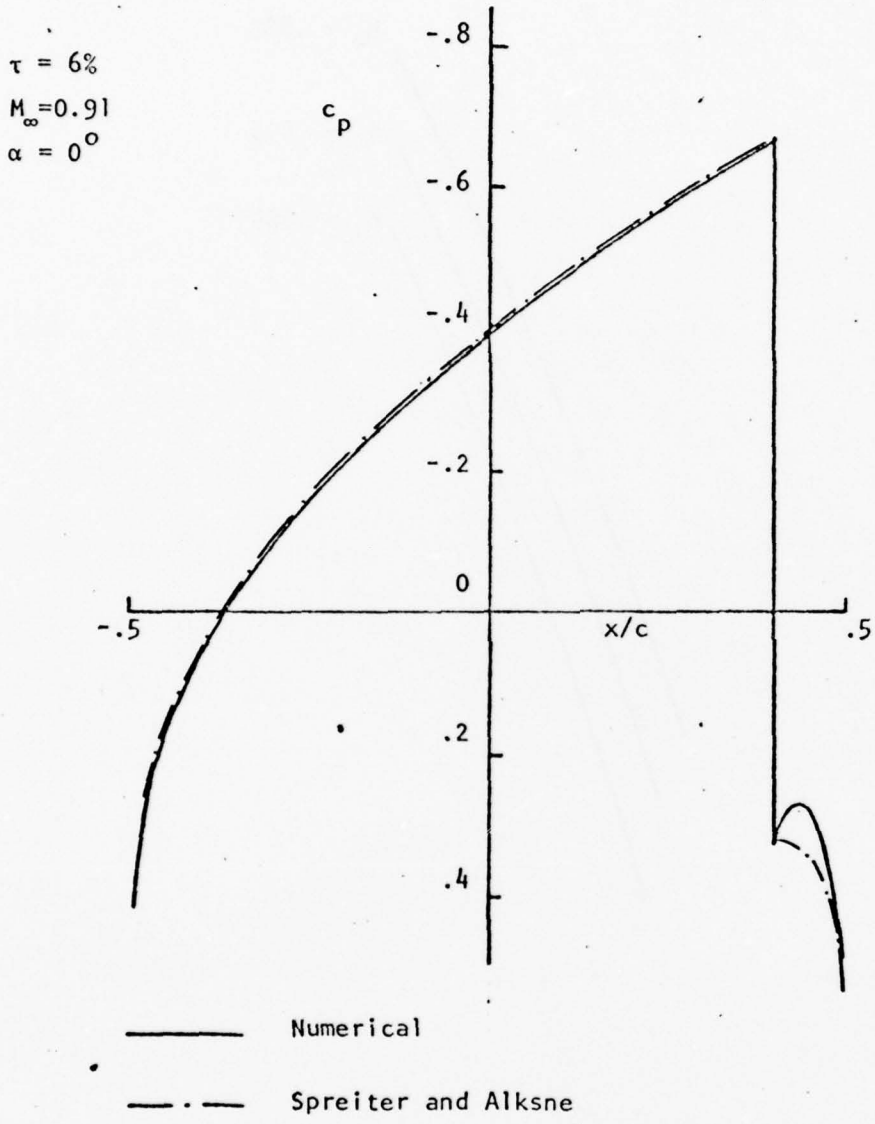

FIGURE 2. PRESSURE DISTRIBUTION OVER A CIRCULAR ARC AIRFOIL. COMPARISON BETWEEN A NUMERICAL SOLUTION AND THE SOLUTION OF SPREITER AND ALKSNE, REFERENCE (15).

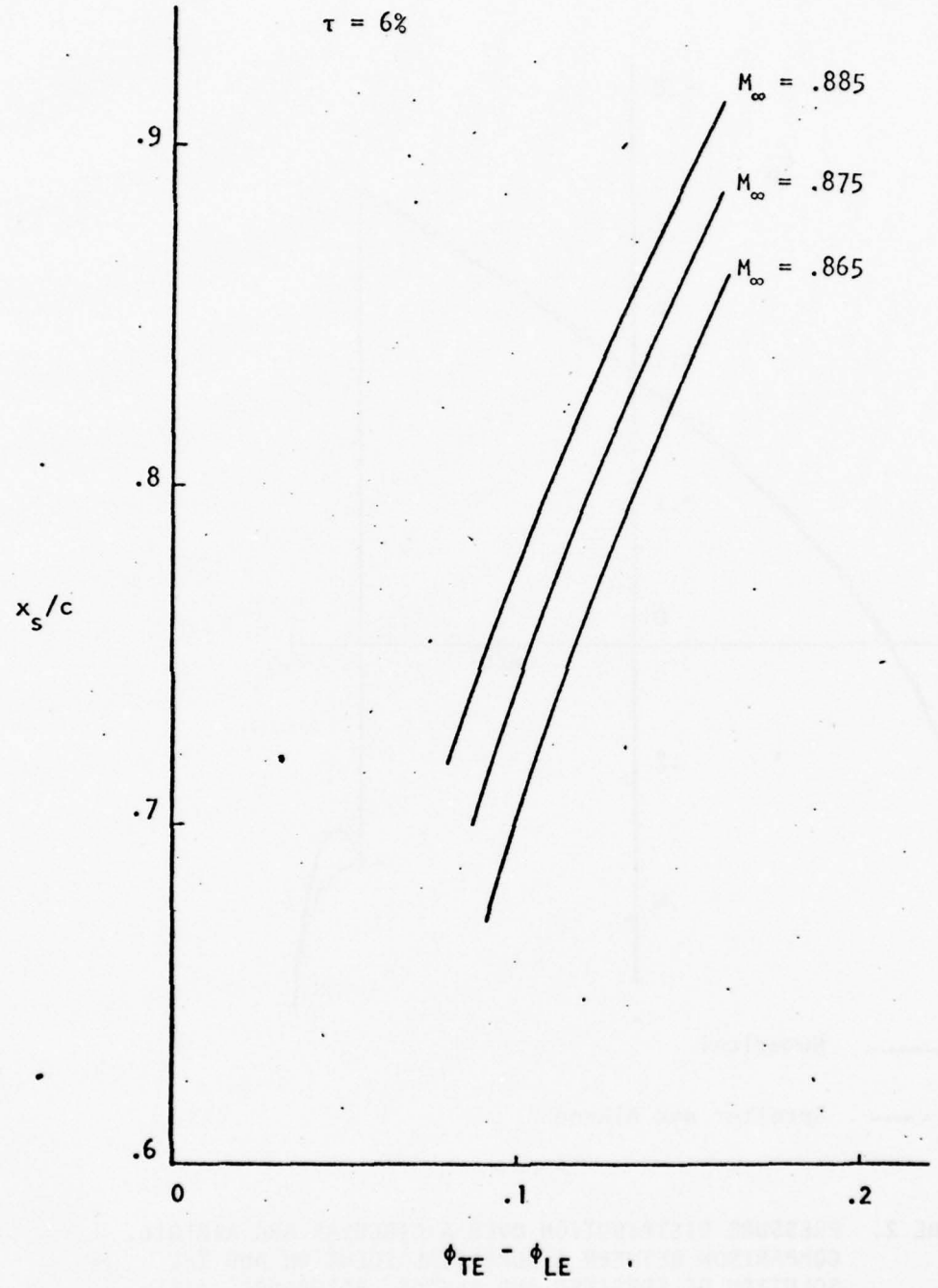

FIGURE 3. DIFFERENCE OF POTENTIAL BETWEEN TRAILING AND LEADING EDGE OF A CIRCULAR ARC AIRFOIL AS FUNCTION OF SHOCK LOCATION AND MACH NUMBER.

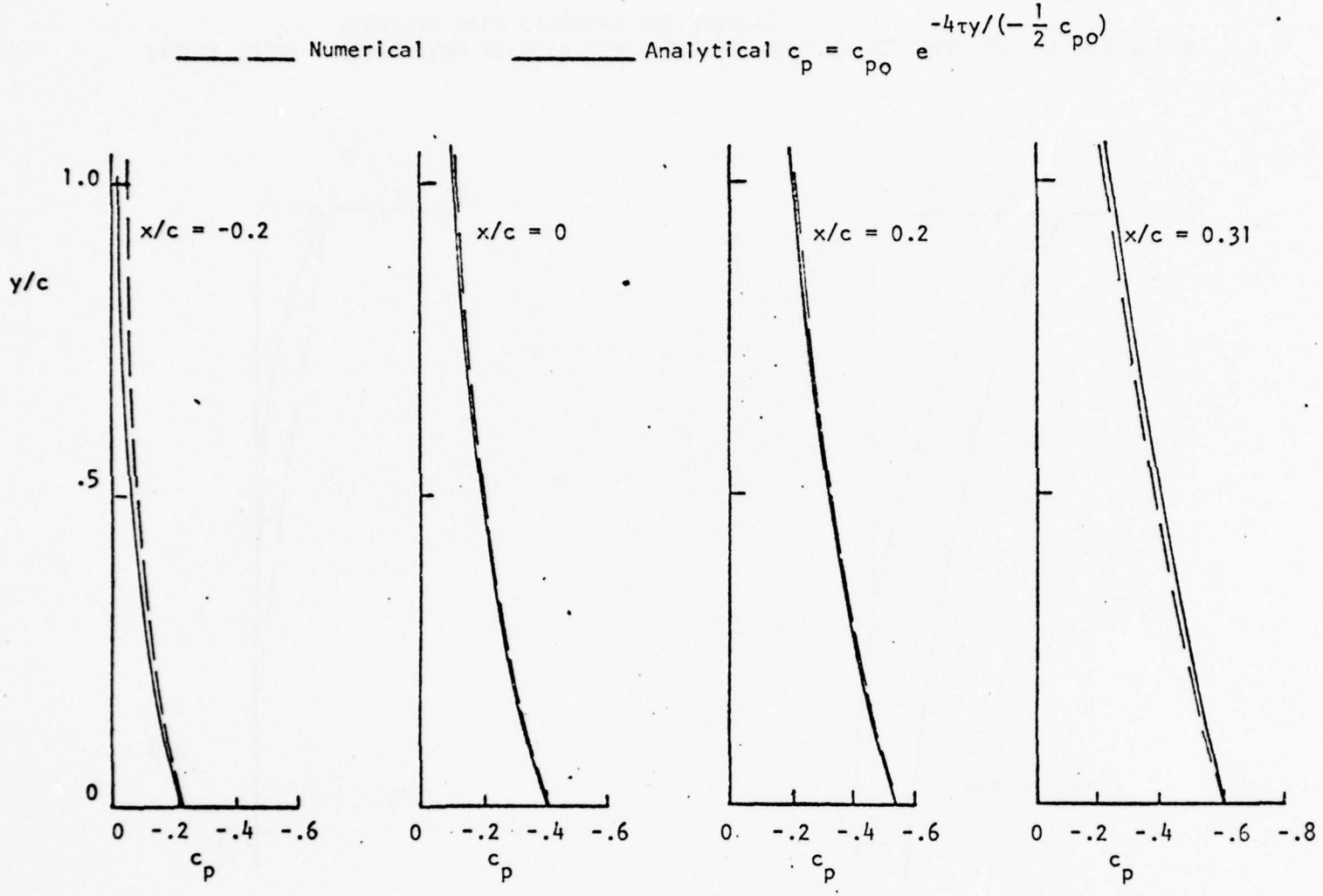

FIGURE (4,a). COMPARISON BETWEEN NUMERICAL AND ANALYTICAL SOLUTION OF MID FIELD VELOCITY OVER CIRCULAR ARC AIRFOIL.

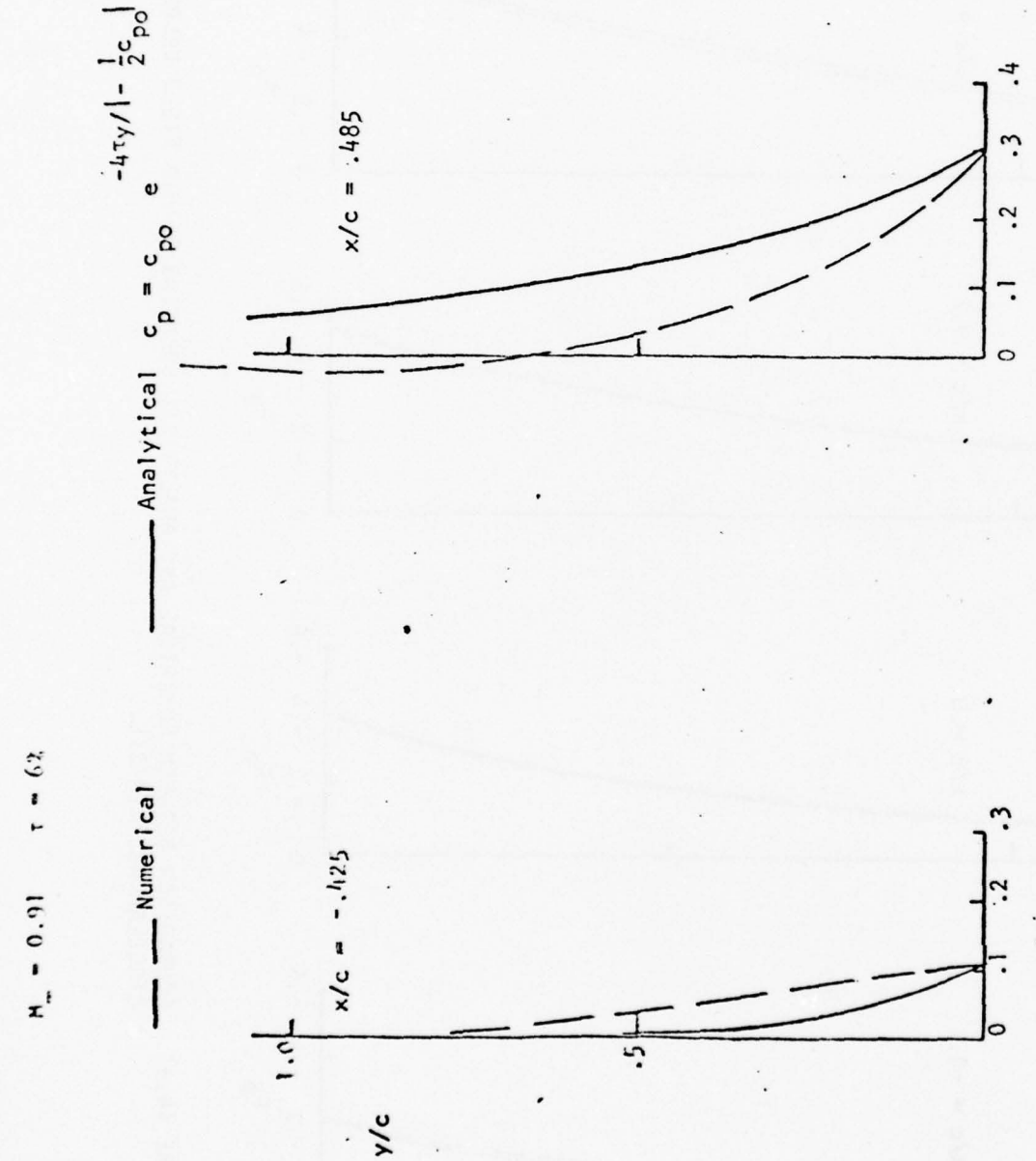

FIGURE (4,b). COMPARISON BETWEEN NUMERICAL AND ANALYTICAL SOLUTION OF MID FIELD VELOCITY OVER CIRCULAR ARC AIRFOIL.

the relationship

$$D = 2\int_{-1/2}^{1/2} 2\tau(1/4-x^2)\,dx + (\gamma+1)\int_{-\infty}^{\infty} u_o^2 \int_0^{\infty} e^{-3\tau y/|u_o|}\,dy\,dx$$

$$\frac{2\tau}{3} + \frac{\gamma+1}{8\tau}\int_{-\infty}^{\infty} |u_o|^3\,dx.$$

The evaluation of the integral is performed numerically and the value of D determined. The strength of the doublet is now taken to correspond to that of a new circular arc airfoil of thickness τ^* for which

$$D = \frac{2\tau^*}{3}$$

Hence, the new airfoil thickness is provided by the expression

$$\tau^* = \tau + \frac{3}{2}\frac{\gamma+1}{8\tau}\int_{-1/2}^{1/2} |u_o|^3\,dx.$$

The airfoil of thickness τ^* satisfies the far field potential. It is, however, of interest to compare with the numerical results the normal velocity perturbation induced at closer distances from the airfoil (in correspondence to possible locations of tunnel walls) by an airfoil of thickness τ^*. Such a comparison is shown in Figure (5) for a circular arc airfoil which has an original thickness of 6% and which, with the inclusion of the nonlinear effects embodied by the double integral, has a thickness $\tau^*=0.13$. The analytical results with $\tau^*=0.13$ are, necessarily, antisymmetric with respect to the airfoil center (x=0 position) in contrast to the actual physical situation reflected by the

$M_\infty = 0.91$

$y/c = 1.585$

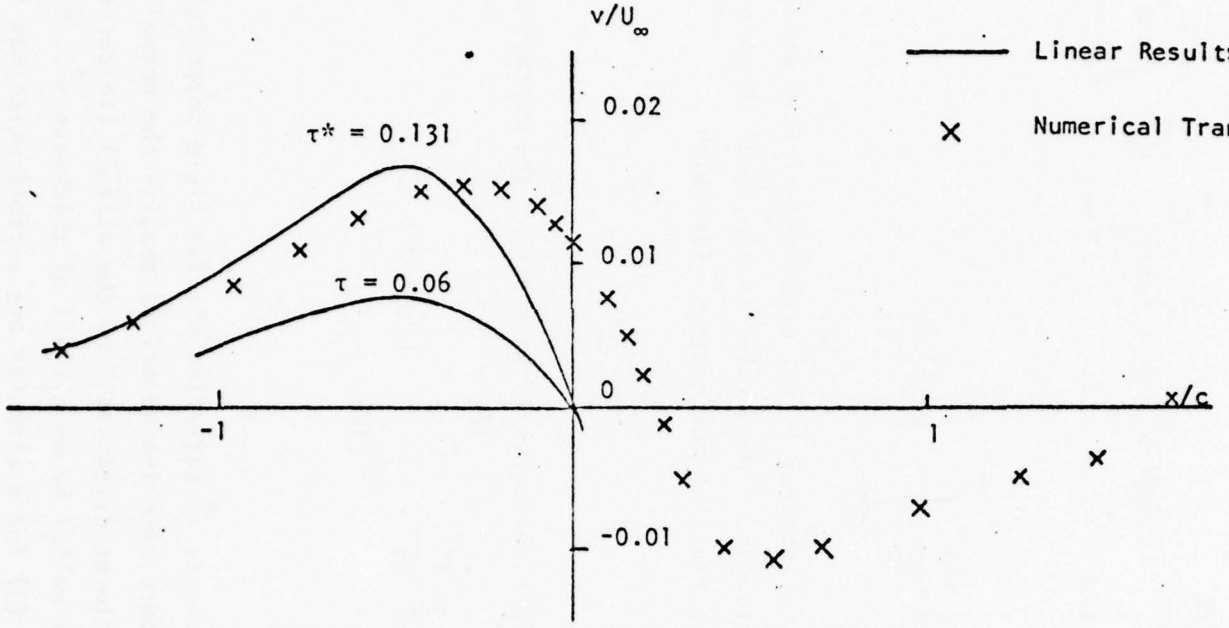

FIGURE 5. COMPUTATIONS OF NORMAL PERTURBATION VELOCITY ALONG A LINE ABOVE A CIRCULAR ARC AIRFOIL.

numerical results. The level of the perturbation is, however, in reasonable agreement with the numerical results and much closer to these than the analytical result based on the value of τ=0.06.

It remains now to determine the interference potential produced by the wall constraints. Several computations have been performed parametrically in terms of free-stream Mach number and tunnel height for tunnels with solid, porous and slotted walls. For a porous or solid wall, the interference potential is provided by Equation (A,8) of the Appendix; for a slotted wall by Equation (A,13). For circular arc airfoils the integrals of Equations (A,9), (A,10) and (A,14) can be calculated in closed form. The integrals (in the variable p) in (A,8) and (A,13) have been, on the other hand, computed numerically. Once the difference of the interference potential between airfoil trailing edge and leading edge is computed, i.e. $\Delta\phi'=\phi'_{TE}-\phi'_{LE}$, the difference is added to the value of $\Delta\phi$ pertaining to the original shock location x_s, and the new shock location is then determined from Figure (3).

Shown in Figure (6) is the effect of a solid wall on shock location for a 6% thick circular arc airfoil at M_∞=0.91 in a tunnel of height twice the airfoil chord, i.e., h/c=2. (The free air results, taken as a reference, are those given by Kraft[7].) Also shown in the figure, for comparison, are the results obtained by Kraft[7] by the integral equation method based on the solution of the transonic small disturbance equation. Reasonable agreement between the present results and those of Kraft can be observed. Shown in Figure (7) are typical results pertaining to the same airfoil in a tunnel with porous walls for the two values of $T\equiv 1/R$=4 and 10. Good agreement with the results of Kraft[7] can again be observed. Finally, the results given in Figure (8) refer to the same airfoil in a slotted tunnel with h/c=1.5 and 2.00 and with a slot parameter K=0.5. As indicated in Reference (14), a value of K=0.5 corresponds to the slotted tunnel of the Flight Dynamics Laboratory, Wright-Patterson air Force Base, the facility from which the experimental data presented previously in Figure (1) were taken. Thus, the results of Figure (8), when referred to the experimental data of Figure (1), seem to provide again a reasonable prediction of shock displacement (upstream displacement in this particular case) under the effect of wall interference.

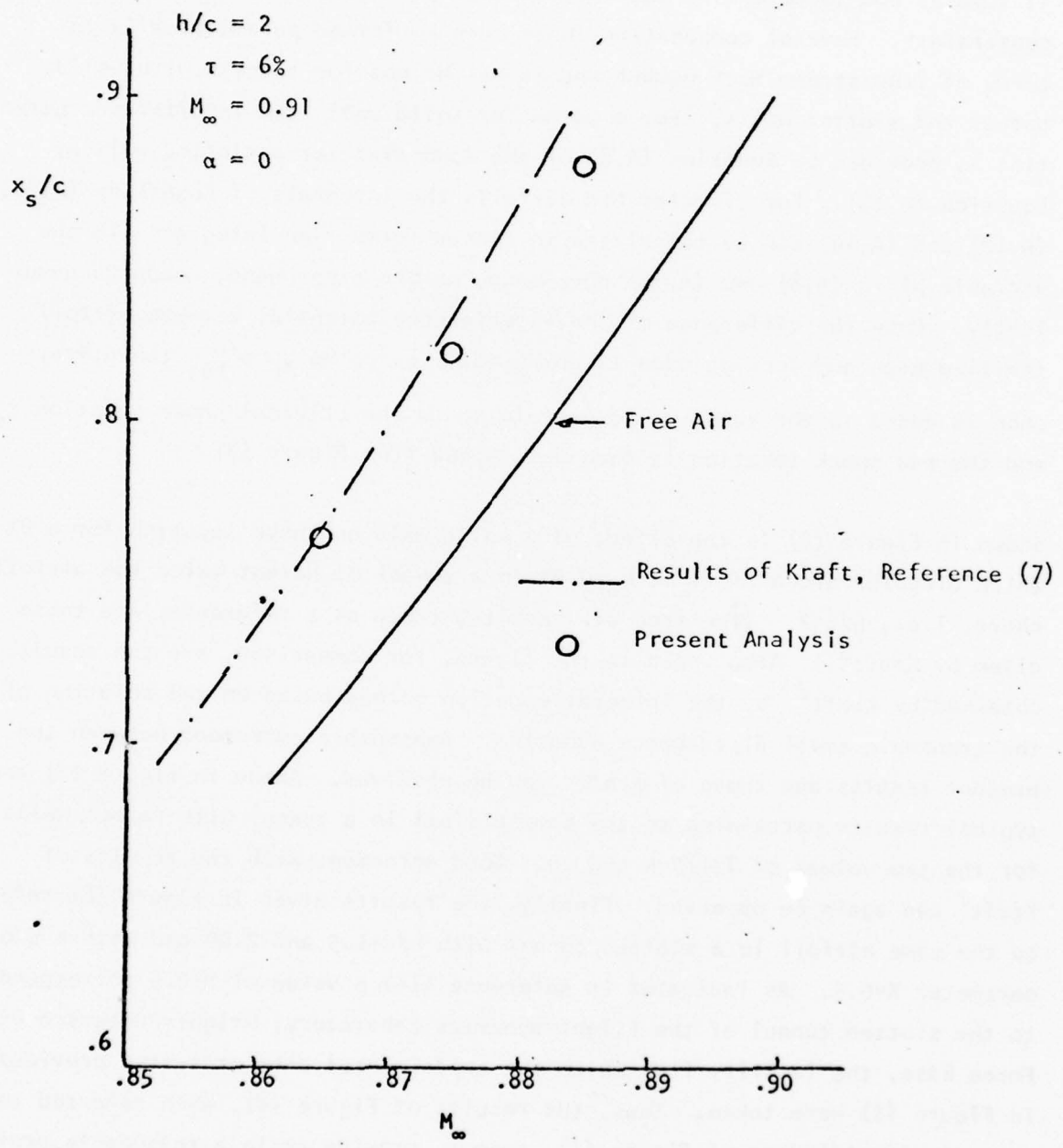

FIGURE 6. EFFECT OF SOLID WALL ON SHOCK LOCATION OVER CIRCULAR ARC AIRFOIL

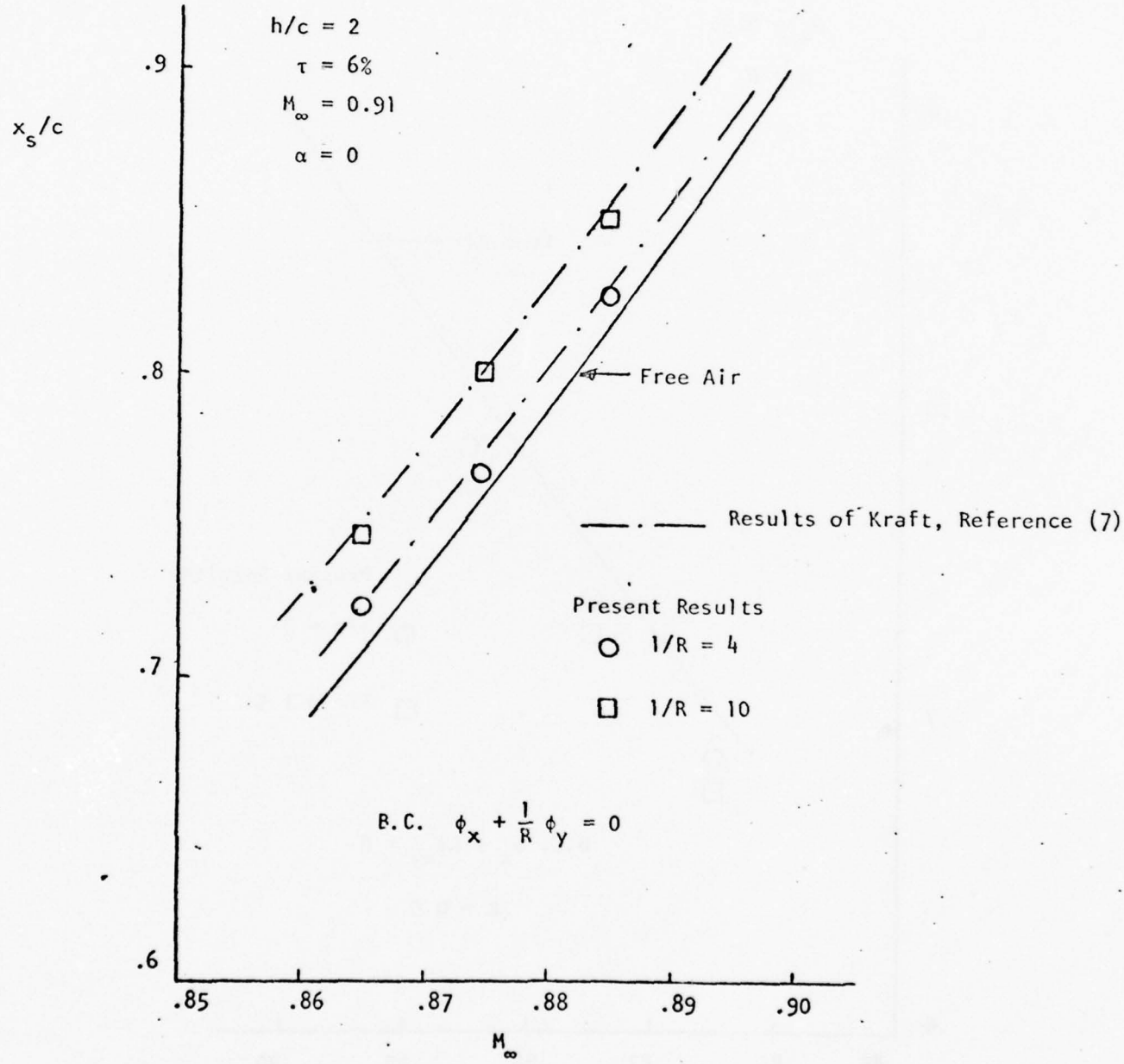

FIGURE 7. EFFECT OF POROUS WALL ON SHOCK LOCATION OVER CIRCULAR ARC AIRFOIL

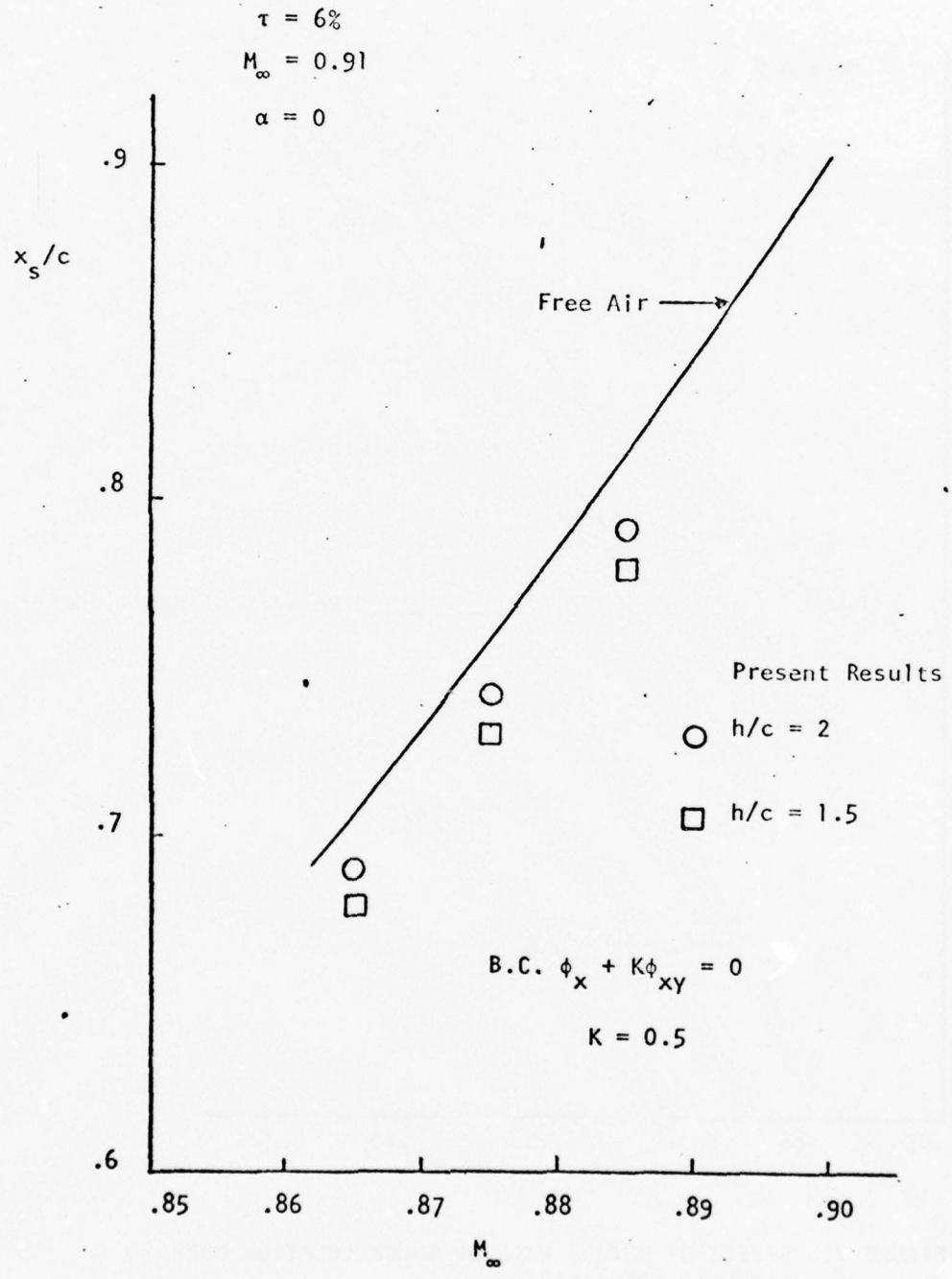

FIGURE 8. EFFECT OF SLOTTED WALL ON SHOCK LOCATION OVER CIRCULAR ARC AIRFOIL

The validity and extension of the method to other configurations depends evidently on the validity and generality of the assumptions that have been introduced. One assumption is that wall interference does not much change the pressure distribution upstream of the shock. The results of Figure (9), taken from Reference (7), which show typically the effects of a solid wall on the pressure distribution over a NACA 12 airfoil, seem to indicate that the assumption has not a general validity and that the wall interference on the pressure distribution is configuration dependent. However, even under the conditions of the figure, it seems that the major effect of wall interference is the shift of the shock and, thus, that the procedure can be perhaps invoked for an assessment of first order corrections for general non-lifting airfoils.

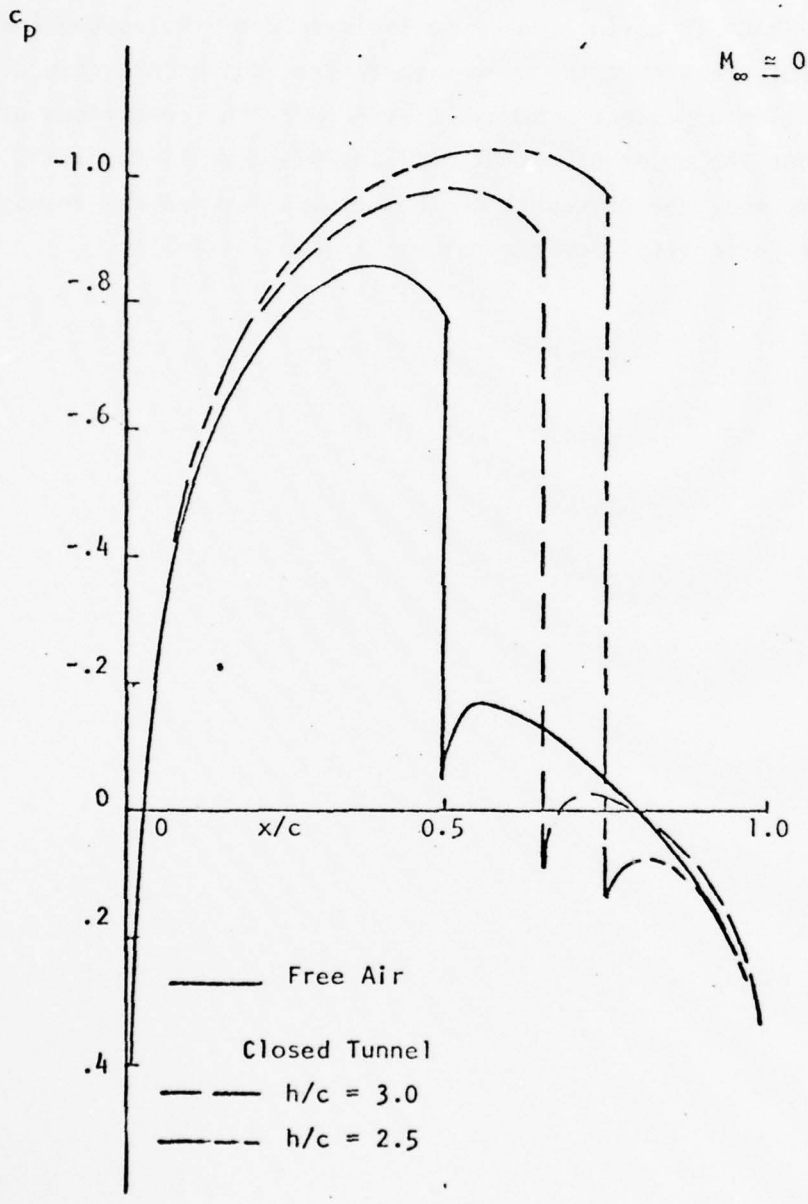

FIGURE 9. EFFECT OF A CLOSED WIND TUNNEL ON PRESSURE DISTRIBUTION OVER A NACA 0012 AIRFOIL, REFERENCE (7).

SECTION III

SHOCK FITTING TECHNIQUE AND DETERMINATION OF BACK PRESSURE EFFECTS ON SHOCK LOCATION

Background

During the past several years, difference formulas have been successfully employed to numerically approximate the differential equations governing a transonic flow field. Successive line overrelaxation (SLOR) is a reliable and efficient procedure to solve the resulting set of simultaneous, algebraic equations, and computer codes using such relaxation schemes have been developed to treat the transonic small disturbance equation. If the flow is supercritical these codes make no distinction for grid points in the vicinity of the shock but rather allow the shock wave to naturally develop in the course of the iteration procedure as a discontinuity smeared over a few mesh points. Results with embedded shocks do, however, indicate a shock pressure rise on the surface consistently less than the theoretical value.

Murman[12] attempted to resolve the discrepancy by the introduction of a shock point operator. At a supersonic-subsonic transition, the x difference operator at the first subsonic point downstream of the shock is replaced by the sum of the x-differences for the elliptic and hyperbolic operators. Murman then demonstrated that the correct normal shock jump condition occurs over three mesh intervals. For the case of an infinite oblique shock, the shock point operator can reproduce the correct shock jump condition at upstream and downstream flow positions which are several grid points removed from the shock position (under the stipulation that the oblique shock passes through two grid points, i.e., $(dx/dy)_s=\Delta x/N\Delta y$, where N is an integer, or $\Delta x,\Delta y$ arbitrary in the limiting case of an infinitesimally refined grid network).

The shortcomings of Murman's shock point operator are discussed by Hafez and Cheng[13], viz. (1) the requirement that grid arrangement be such that $\Delta x/\Delta y=N(dx/dy)_s$ is not readily obtainable for an arbitrary grid, (2) the discontinuity in ϕ_y across the shock is computed in a manner that will, in most cases, underestimate ϕ_y on the upstream side of the shock and (3) the correct supersonic-subsonic transition cannot be accomplished in a single jump but requires a few grid points.

Hafez and Cheng[13] suggested an improved shock fitting technique, which satisfies the Rankine-Hugoniot condition and which defines more exactly the shock position even with coarser grids. The shock fitting procedure modifies the difference equations mainly in the treatment of grid points near the shock. The original difference equation is replaced by the difference form of the jump relations at the point on each horizontal line nearest to the shock on the downstream side, and backward extrapolation is used to evaluate the potential at the nearest grid point along each vertical on the upstream side. For a plane-normal shock, the above shock fitting procedure collapses to Murman's shock operator formulation. In general, however, the two procedures do not agree because of the difference in which the jump in transverse velocity ϕ_y is computed.

The shock fitting procedure of Hafez and Cheng does, however, apply to the shock jump conditions between neighboring grid points rather than at the actual shock position. It is the present intent to further refine the shock fitting technique, removing this discrepancy by calculating the shock position within the iteration procedure as a discrete discontinuity across which the transonic approximation of the Rankine-Hugoniot conditions apply.

• Formulation

The transonic small disturbance approximations of the Rankine-Hugoniot conditions are

$$-(1-M_\infty^2) + \frac{\gamma+1}{2}(\phi_{x_1}+\phi_{x_2}) = \frac{\langle\phi_y\rangle^2}{\langle\phi_x\rangle^2} \qquad (6,a)$$

$$\frac{\langle\phi_y\rangle}{\langle\phi_x\rangle} = -\left(\frac{dx}{dy}\right)_s \qquad (6,b)$$

where $\langle\ \rangle$ signifies the jump, and the subscripts 1 and 2 represent the upstream and downstream side of the shock, respectively. The first equation is the transonic shock polar and the second equation expresses the continuity of tangential velocity across the shock. The latter condition can be immediately satisfied by requiring the potential to be continuous across the shock. The line relax-

ation procedure to which the shock fitting method will be applied is that of Murman[11,12]. The derivation of the shock fitting procedure closely resembles that of Hafez and Cheng[13].

For a supersonic-subsonic shock transition, the modifications in the difference equations are found mainly in the treatment of the grid points on each horizontal line nearest to the shock on the downstream side, and of the nearest grid point along each vertical across the shock. These points, labelled P and Q, respectively, are shown in Figure (10). Three types of local shock inclination indicated in Figure (10) must be distinguished in treating point P. By examining the elliptic/hyperbolic nature of the grid points about P the type of local shock inclination is determined. The shock inclination having been classified as type (a), (b) or (c), its position, á priori known to lie within the interval $P'P$, is calculated by the following procedure. The interval $P'P$ is subdivided into N-1 equally spaced intervals as shown typically in (b) of Figure (10) where P_n, n=1, 2, 3 . . . , N is a general point within $P'P$. Assuming the point P_n to correspond to the shock position, values of the potential and of the x-velocity component at the upstream side of the shock, $(\phi_1)_{P_n}$ and $(u_1)_{P_n}$, respectively, are obtained by forward extrapolation from upstream grid points. Continuity of the potential across the shock yields the potential $(\phi_2)_{P_n}$ on the downstream side of the shock, whereas Equation (6,a) yields the x-velocity component, $(u_2)_{P_n}$ on the downstream side of the shock*. The first order Taylor expansion about the downstream side of the shock

$$\tilde{\phi}_P = \phi(x_{P_n}, y_P) + (\phi_x)_{P_n} (x_P - x_{P_n}) \tag{7}$$

supplies a potential at P, denoted by $\tilde{\phi}_P$. The error function $E(x_{P_n}) = \tilde{\phi}_P - \phi_P^{(\nu-1)}$, where $\phi_P^{(\nu-1)}$ is the potential at P at the previous iteration, is formed and the position, $x_P = x_s$, in the interval $P'P$, where the error function is zero, is identified as the shock location.

*To compute the RHS of Equation (6,a), values obtained at the previous iteration step are used, with the ϕ_x's and the ϕ_y's evaluated by central differences at A and B, and D and C, respectively, in the manner shown in (a), (b) and (c) of Figure (10).

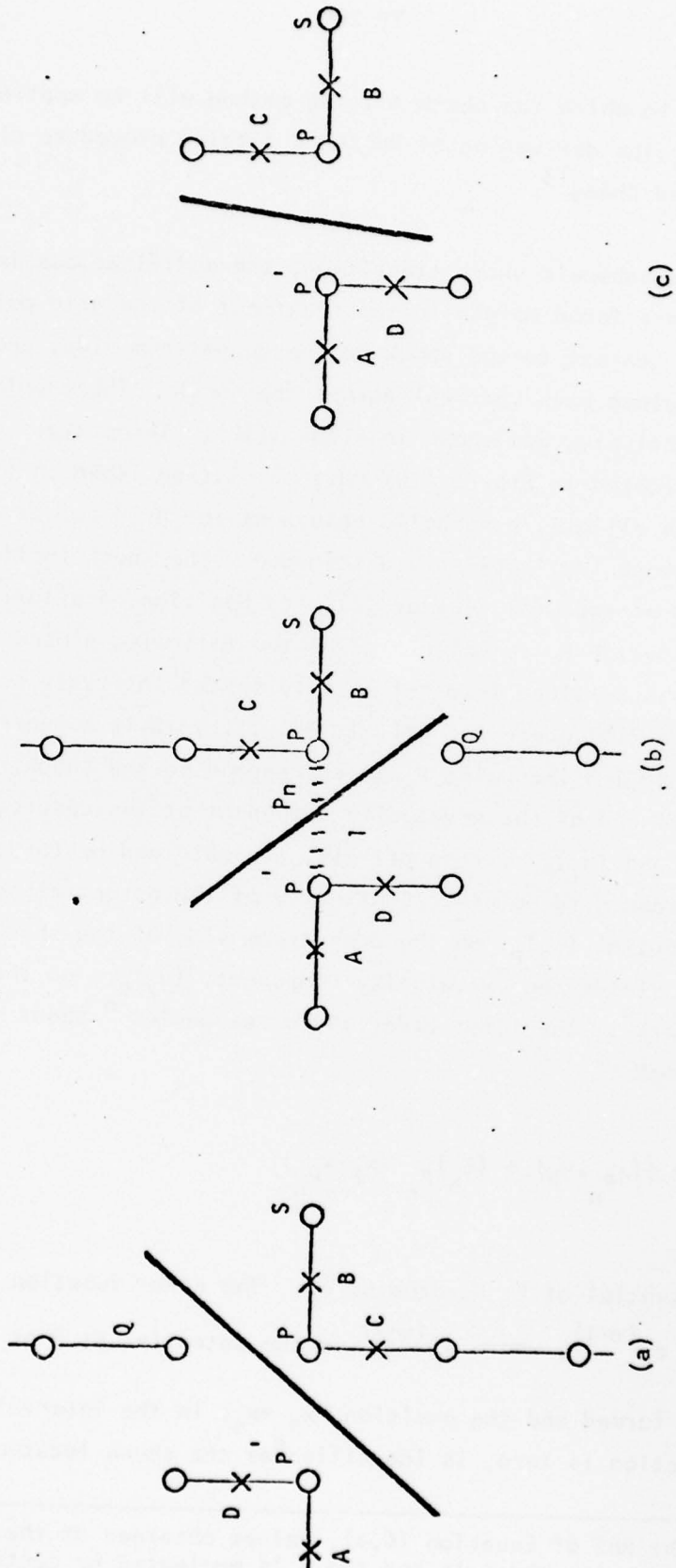

FIGURE 10. GRID POINTS ARRANGEMENT FOR SHOCK FITTING TECHNIQUE

The difference scheme at P is written so as not to cross the shock when approximating derivatives by finite differences.* The original difference equation for the upstream point Q must also be redefined in cases (a) and (b), because one of the five points in the backward hyperbolic operator lies on the other side of the shock. The needed data are supplied by forward (downstream) extrapolation to P from three upstream points.

For a supercritical flow the elliptic and hyperbolic regions, identified by

$$\left[1 - M_\infty^2 - (\gamma+1)M_\infty^2\phi_x\right] \begin{matrix} < 0 \text{ hyperbolic} \\ > 0 \text{ elliptic,} \end{matrix}$$

are separated by a sonic boundary and by a shock. For flows accelerating through a sonic boundary the difference form of the equations of the original relaxation scheme is retained. For flows decelerating through a shock, however, the difference equations of the original scheme are replaced by the difference formulation described above. Following Reference (13), to distinguish the shock from the sonic line, ϕ_x is required to decrease by a prescribed fraction of the grid size in a supersonic-subsonic transition.

Numerical Results

The present shock fitting procedure has been investigated intensively and numerical results have been compared with those obtained by applying the method of Hafez and Cheng.[13] (A numerical code based on the analysis of Hafez and Cheng has also been constructed to allow direct comparison of the two methods.) A typical comparison is provided by Figure (11) which shows the pressure distribution over a 6% thick circular arc airfoil at $M_\infty = 0.87$. The grid network consists of 41 x 20 points. The two sets of results are those obtained after 1200 relaxation steps. Shown in Figure (12) is the algorithm providing the shock location within two neighboring points. Plotted in the figure is the error function $E(\xi_s)$ for two points above a 6% thick circular arc airfoil

*The potentials at P_η, P and S are used to form the difference approximations of the x-derivatives, whereas central differences at Q (for shock inclination types (a) and (b) of Figure (10)) or at P (for shock inclination type (c) of Figure (10)) are used to approximate the y-derivatives.

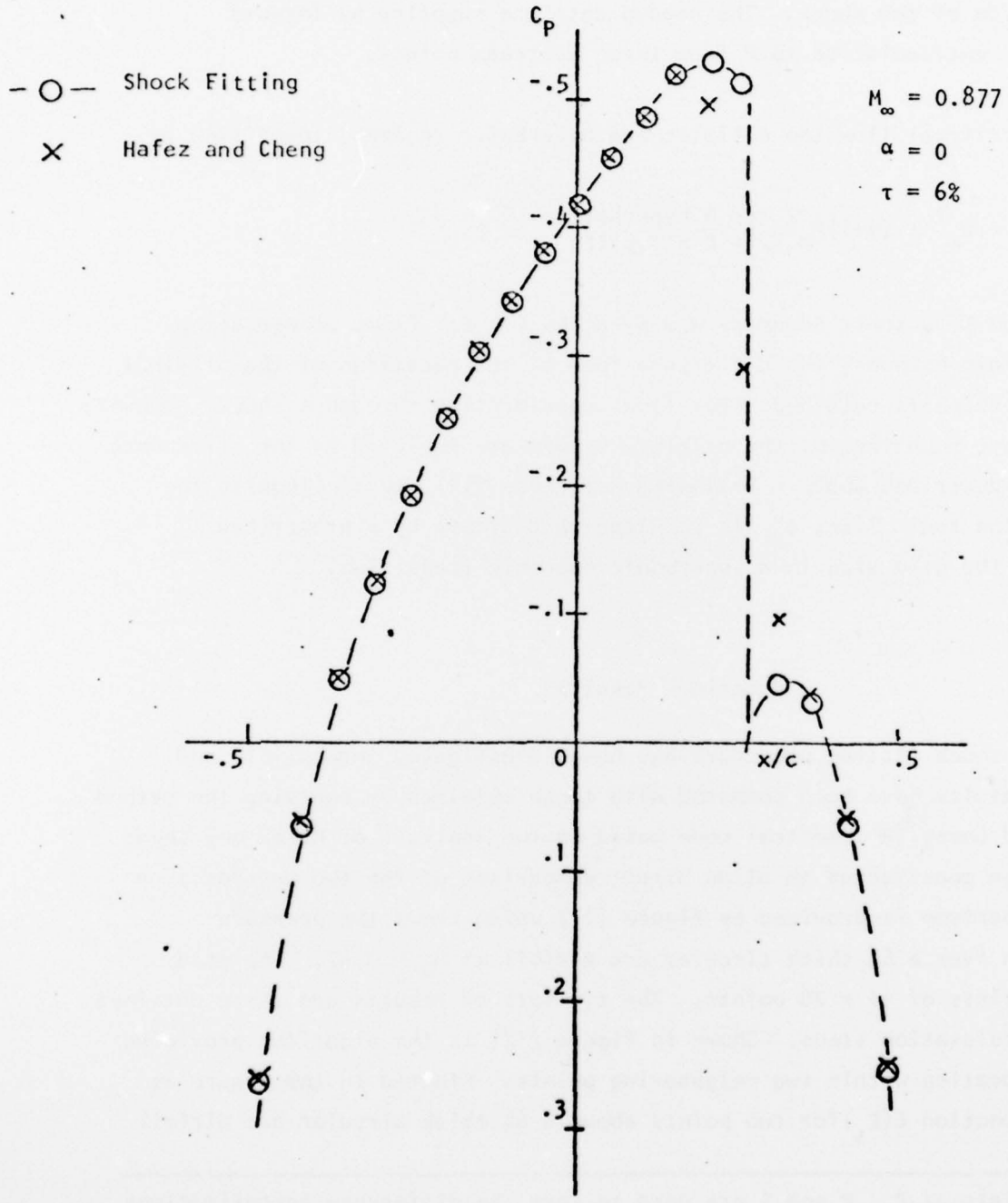

FIGURE 11. COMPARISON BETWEEN PRESENT SHOCK FITTING SOLUTION WITH SOLUTION BY HAFEZ AND CHENG, REFERENCE (13)

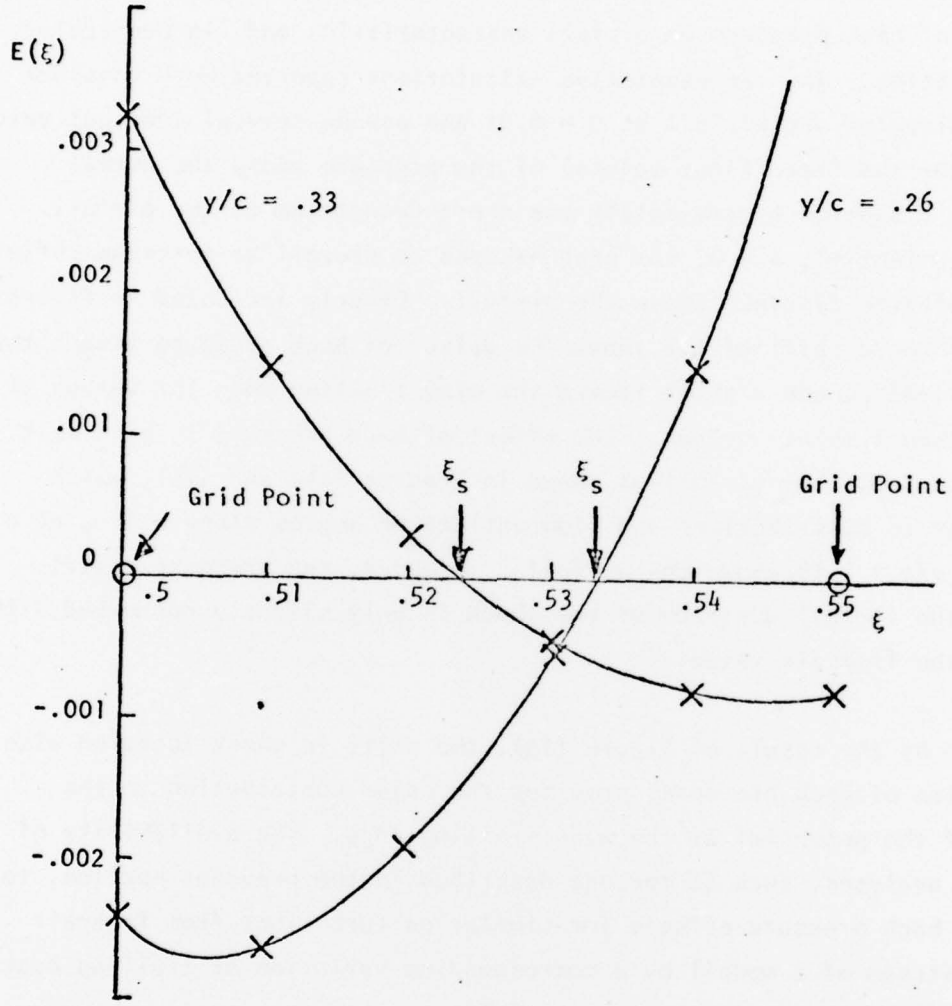

FIGURE 12. DETERMINATION OF SHOCK POSITION BETWEEN ADJACENT GRID POINTS

at $M = 0.94$. The shock location is identified by the values of ξ_s for which $E(\xi_s) = 0$. (ξ is the stretched x-coordinate in the computational space.)

Systematic calculations have then been performed with the program to ascertain the effects of back pressure on airfoil characteristics and, in particular, on shock location. The representative calculations reported here consider a 6% thick circular arc airfoil at $M = 0.91$ and assume several constant values (different for the free flight values) of the pressure along the normal direction at a station approximately one chord downstream of the airfoil. Unperturbed potential, $\phi = 0$, has been assumed to prevail at upstream infinity and at an infinite distance above the airfoil. Clearly indicated in Figure (13) are a forward shift of the shock for values of back pressure larger than the free-air values and a shift toward the wing trailing edge for values of C_p smaller than free-air values. The effect of back pressure is also felt in the region above the airfoil as shown in Figures (14) and (15), which present pressure distributions and flow deflection angles along a line at a distance of $y/c = 1.58$ above the airfoil. However, the pressure distributions on the airfoil upstream of the shock is only slightly perturbed with respect to the free-air value.

As indicated by the result of Figure (13), the shift in shock location with a perturbation of back pressure, provides the major contribution to the variation of the potential at the wing trailing edge. The availability of approximate analyses, such as the one described in the previous section, to account for back pressure effects (or similar perturbations from free-air values downstream of a model) by a corresponding variation of trailing edge potential would then, again, be very useful.

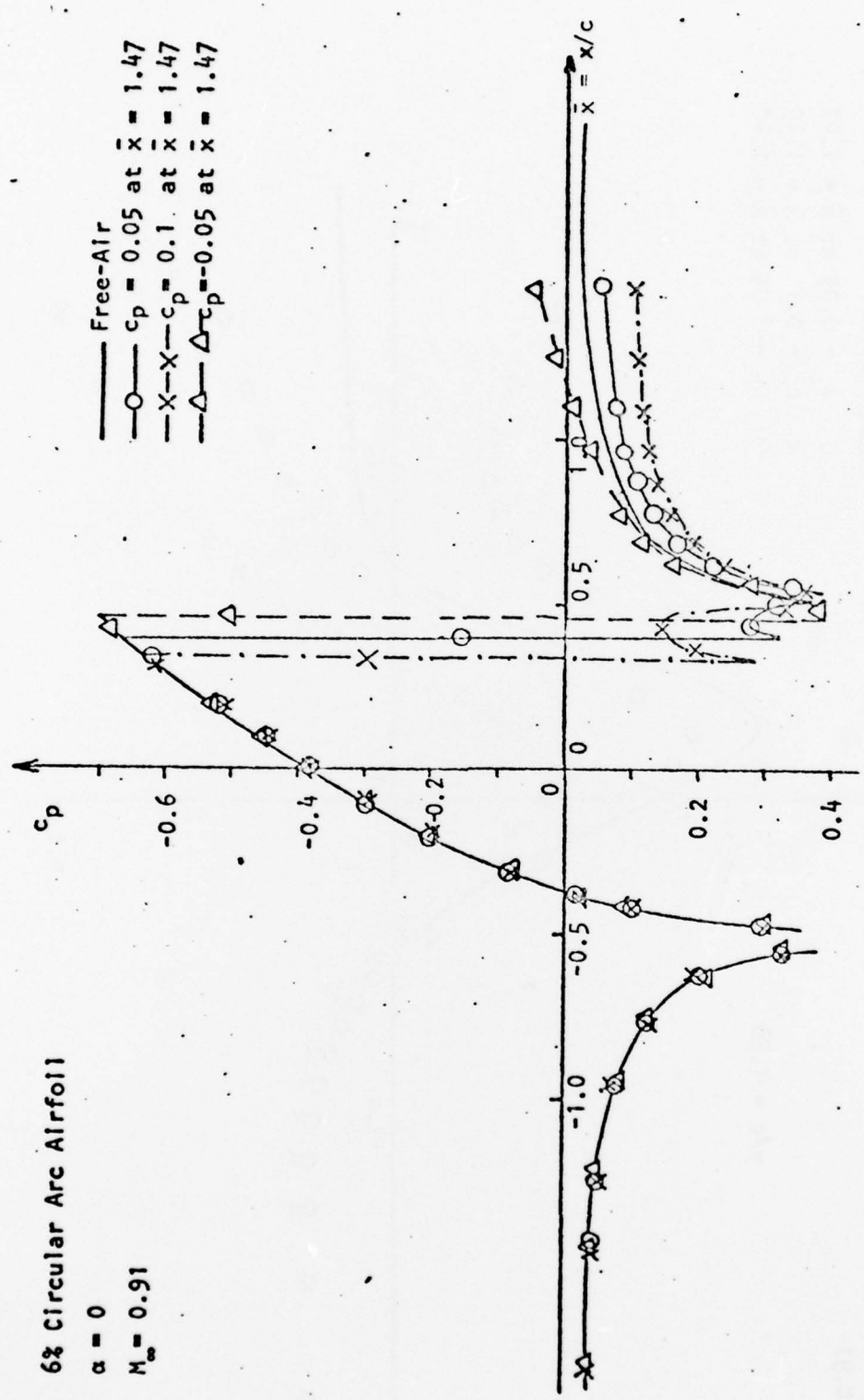

FIGURE 13. EFFECT OF BACK PRESSURE ON SHOCK LOCATION. NUMERICAL RESULTS

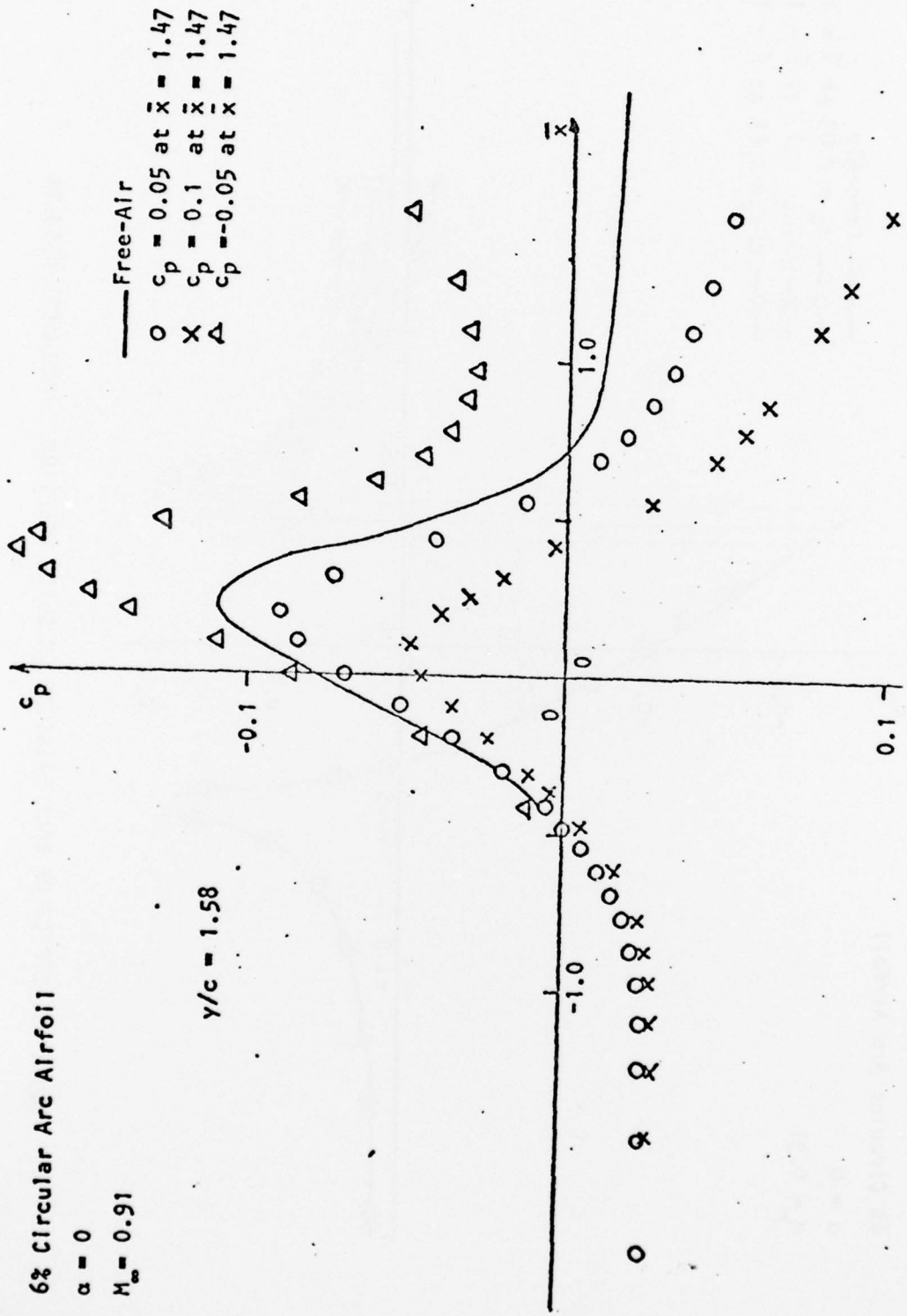

FIGURE 14. PRESSURE DISTRIBUTIONS ALONG LINE y/c = 1.58 FROM AIRFOIL FOR SEVERAL VALUES OF BACK PRESSURE

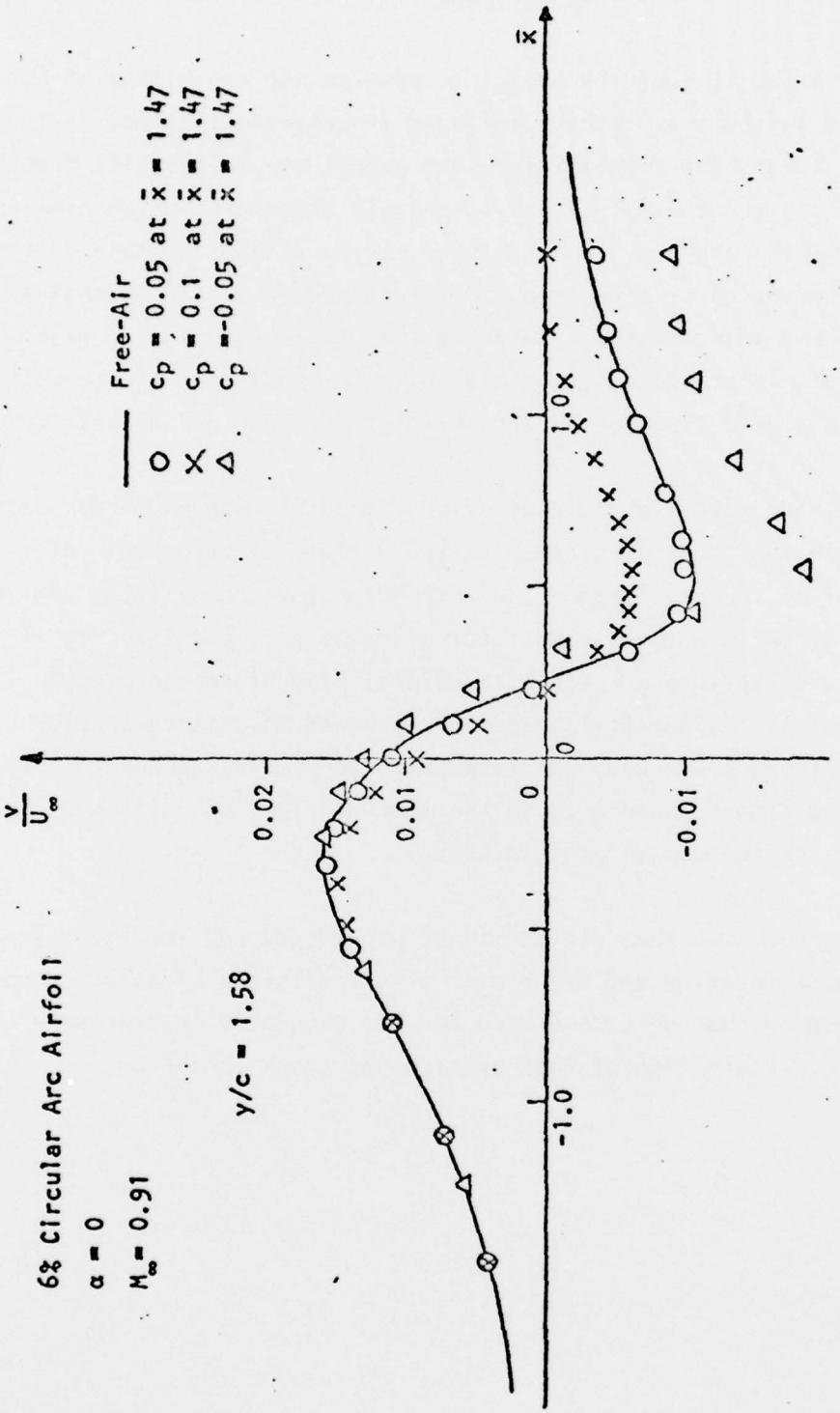

FIGURE 15. FLOW DEFLECTIONS ALONG LINE y/c = 1.58 FROM AIRFOIL FOR SEVERAL VALUES OF BACK PRESSURE

SECTION IV
CONCLUSIONS

In transonic testing it would be useful to possess the capability of correcting the tunnel data in the same fashion followed in subsonic testing. Attempts are now being made to develop capabilities that permit one to quantify transonic wall interference; the concept of correctable interference, which combines tunnel measurements with numerical analyses, is an attempt in this direction. The method suggested here is an even simpler procedure for an approximate determination of tunnel interference. Based on the observation that a major manifestation of wall interference is a shift of shock position, a methodology is presented for the determination of the shift of the shock due to wall constraints.

The feasibility and relative accuracy of the method is proved herein only for simple configurations such as a circular arc airfoil at zero angle of attack. An extension of the concept and of the method to other non-lifting configurations such as airfoils with blunted leading edges, and, possibly, to lifting airfoils, could constitute a worthwhile effort. The present procedure is admittedly approximate, since it is essentially based on a linearization of the nonlinear interference process, but it appears to provide an adequate representation of the flow-phenomena (with the same accuracy of more complex analyses) at least for the cases reported here.

A shock fitting technique has, in addition, been developed for the exact determination of shock location and shape over a supercritical airfoil. A concomitant computer program has been developed and has been used to precisely assess the effect of a perturbation of back pressure on shock location.

APPENDIX A

BLOCKAGE INTERFERENCE BY LINEARIZED SUBSONIC THEORY

The linearized subsonic theory of wall interference for nonlifting, two-dimensional airfoils in tunnels with solid, porous and slotted walls is reviewed here. The present derivation determines the interference potential by following the analysis of Lo[6] for the particular case where the non-linear term is neglected.

The analysis is based on the solution of the linearized equation of subsonic compressible flow

$$(1 - M_\infty^2)\ \phi_{xx} + \phi_{yy} = 0 \tag{A.1}$$

subject to the tangential flow condition at the airfoil surface

$$\phi_y = \tau\, F_x(x) \tag{A.2}$$

where F(x) is the airfoil profile function, and, for the case of a porous wall, to the wall boundary condition, at y = h,

$$\phi_x + T\ \phi_y = 0 \tag{A.3}$$

where T is the porosity parameter. For $T \to \infty$ the solid wall boundary condition, $\phi_y = 0$, is recovered.

The method of Fourier transform is now applied, by taking the Fourier transform of $\phi(x)$,

$$\bar{\phi}(p) = (2\pi)^{-1/2} \int_{-\infty}^{\infty} \phi(x)\, e^{ipx}\, dx, \tag{A.4}$$

to yield the equation

$$-\beta^2 p^2 \bar{\phi} + \bar{\phi}_{yy} = 0 \tag{A.5}$$

and the boundary conditions

$$\bar{\phi}_y = \tau\, f(p) = (2\pi)^{-1/2} \int_{-\infty}^{\infty} \tau \quad F_x\, e^{ipx}\, dx, \qquad \text{at } y = 0 \qquad \text{(A.6)}$$

and

$$-ip\,\bar{\phi} + T\,\bar{\phi}_y = 0, \qquad \text{at } y = 0 \qquad \text{(A.7)}$$

The solution of Equation (A.5), subject to boundary conditions (A.6) and (A.7), in the transform plane is

$$\bar{\phi} = \bar{\phi}_m - \frac{\tau\, f(p)}{\lambda} \frac{(ip + T\lambda)e^{-\lambda h}}{ip \cosh \lambda h + T\lambda \sinh \lambda h} \cosh \lambda y$$

where $\lambda = \beta p$ and where $\bar{\phi}_m$ is the free air solution i.e., $\phi_m = -(\tau\, f(p)/\lambda)e^{-\lambda y}$.

The interference potential in the transform plane, is then given by

$$\bar{\phi}_i = \bar{\phi} - \bar{\phi}_m ,$$

which, by the inverse transform, yields, in the physical plane, the real value potential

$$\phi_i = -\frac{2}{\pi}\left[\int_0^{\infty} dp \quad I_c\, e^{-\lambda h} \quad \frac{\cosh \lambda y}{\lambda} \quad M_c \right.$$

$$\left. + \int_0^{\infty} dp \quad I_s\, e^{-\lambda h} \quad \frac{\cosh \lambda y}{\lambda} \quad M_s \right] \qquad \text{(A.8)}$$

where

$$I_c = (p^2 H + T\lambda\, p^2 G)/D$$

$$I_s = (-T\lambda\, H + p^2 G)\, p/D$$

$$D = H^2 + p^2\, G^2$$

$$H = T\lambda \sinh \lambda h$$

$$G = \cosh\ \lambda h$$

$$\lambda = \beta p$$

and where M_c and M_s are related to the airfoil geometry through the integrals

$$M_c = \int_{-1/2}^{1/2} F(\xi)\ \cos p\ (x-\xi)\, d\xi \qquad (A.9)$$

and

$$M_s = \int_{-1/2}^{1/2} F(\xi) \sin p\ (x-\xi)\, d\xi \qquad (A.10)$$

In the case of a tunnel with slotted walls, the wall boundary condition is usually given by the homogeneous form

$$\phi_x + K\ \phi_{xy} = 0 \qquad (A.11)$$

where K is the slot parameter. For convenience, the integrated form of Equation (A.11) is used here, i.e., the form

$$\phi + K \phi_y = 0 \qquad \text{at } y = h \tag{A.12}$$

which implies zero perturbation potential at upstream infinity. Again by using the Fourier transform (A.4), the solution of Equation (A.5) subject to the boundary condition (A.6) at the airfoil surface, and to the boundary condition

$$\bar{\phi} + K \bar{\phi}_y = 0 \qquad \text{at } y = h$$

yields, in the transform plane, the interference potential

$$\bar{\phi}_i = \frac{\tau f}{\lambda} \left\{ \frac{(1-\lambda K)e^{-\lambda h} \, 2 \cosh \lambda y}{(1+\lambda K)e^{\lambda h} + (1-\lambda K)e^{-\lambda h}} \right\}$$

By the inverse transfrom, we then obtain, in the physical plane, the interference potential

$$\phi_i = \frac{\tau}{\pi} \int_{-\infty}^{\infty} p \, \frac{(1-\lambda K)e^{-\lambda h} \, 2 \cosh \lambda y}{(1+\lambda K)e^{\lambda h} + (1-\lambda K)e^{-\lambda h}} \, M \, dp \tag{A.13}$$

where

$$M = \int_{-1/2}^{1/2} F(\xi) \sin p (\xi - x) \, d\xi \tag{A.14}$$

REFERENCES

1. Murman, E. M. and Cole, J. D., "Calculation of Plane Steady Transonic Flows," AIAA Jrl, Vol. 9, No. 1, January 1971.

2. Ferri, A. and Baronti, P., "A Method for Transonic Wind Tunnel Corrections," AIAA Jrl, Vol. 11, No. 1, January 1973.

3. Sears, W. R., "Self Correcting Wind Tunnels," 16th Lanchester Lecture to the Royal Aeronautical Society, May 1973, also Calspan Corporation Report KR-5070-A-2, Buffalo, NY, July 1973.

4. Kemp, W. B., Jr., "Toward the Correctable Transonic Wind Tunnel," AIAA 9th Aerodynamic Testing Conference, Arlington, Texas, June 1976.

5. Sears, W. K., Vidal, R. I., Erickson, T. C. and Ritter, A., "Interference-Free Wind Tunnel Flows by Adaptive-Wall Technology," ICAS Paper No. 76-02. 10th Congress of the International Council of the Aeronautical Sciences, Ottawa, Canada, October 1976.

6. Lo, C. R., "Application of Linearized Transonic Theory to Tunnel Blockage Interference," AEDC-TR-74-65, September 1974.

7. Kraft, E. M., "An Integral Equation Method for Boundary Interference in a Perforated-Wall Wind Tunnel at Transonic Speeds," AEDC-TR-76-43, April 1976.

8. Kraft, E. M. and Lo, C. F., "Analytical Determination of Blockage Effects in a Perforated-Wall Transonic Wind Tunnel," AIAA Jrl, Vol. 15, No. 4, April 1977.

9. Laughrey, J. A., Richey, G. K. and Ferri, A., "Data Variance Due to Different Testing Techniques," AGARD-AG-208, October 1975.

10. Baronti, P. and Ferri, A., "On the Development of Interference-Free Transonic Wind Tunnels," ATL TR 223, December 1975.

11. Weeks, T. M., "Reduction of Transonic Slotted Wall Interference by Means of Slot Contouring," AFFDL-TR-74-139, March 1975.

12. Murman, E. M., "Analysis of Embedded Shock Waves Calculated by Relaxation Methods," AIAA Jrl, Vol. 12, No. 5, May 1974.

13. Hafez, N. M. and Cheng, H. K., "Convergence Acceleration and Shock Fitting for Transonic Aerodynamics Computations," University of Southern California, School of Engineering, Report USCAE 132, April 1975.

REFERENCES (Continued)

14. Baronti, P., Elzweig, S., Ruger, C., and Weeks, T. M., "Experimental and Analytical Investigation of a Wing Profile in a Slotted Transonic Tunnel," ATL TR 222, November 1975.

15. Spreiter, J. R. and Alksne, A. Y., "Thin Airfoil Theory Based on Approximate Solution of the Transonic Flow Equation," NACA Report 1359, 1958.

16. Spreiter, J. R. and Alksne, A. Y., "Theoretical Prediction of Pressure Distributions on Nonlifting Airfoils at High Subsonic Speeds, NACA Report 1217, 1955.